Two-photon absorption by spectrally shaped entangled photons

Hisaki Oka*
Niigata University, 8050 Ikarashi 2-no-cho, Nishi-ku, Niigata 950-2102, Japan

(Received 5 December 2017; published 12 March 2018)

We theoretically investigate two-photon excitation by spectrally shaped entangled photons with energy anticorrelation in terms of how the real excitation of an intermediate state affects two-photon absorption by entangled photons. Spectral holes are introduced in the entangled photons around the energy levels of an intermediate state so that two-step excitation via the real excitation of the intermediated state can be suppressed. Using a three-level atomic system as an example, we show that the spectral holes well suppress the real excitation of the intermediate state and recover two-photon absorption via a virtual state. Furthermore, for a short pulse close to a monocycle, we show that the excitation efficiency by the spectrally shaped entangled photons can be enhanced a thousand times as large as that by uncorrelated photons.

DOI: 10.1103/PhysRevA.97.033814

I. INTRODUCTION

Two-photon absorption (TPA) using entangled photons has recently attracted much attention because it has potential applications to next-generation technologies in the chemical and biological fields such as optical spectroscopy [1–6], quantum coherent tomography [7,8], and the coherent control of molecules [9,10]. Generally, the realization of efficient TPA requires the simultaneous absorption of two photons. For entangled photons, however, this can be automatically achieved because they have an inherent coincidence based on the quantum correlation, which does not exist in classical light. With the use of entangled photons, though seemingly contradictory, TPA by low-intensity light with a high two-photon flux density can be possible. In fact, the enhancement of the two-photon transition by entangled photons has been theoretically predicted [11–14] and observed experimentally, e.g., in the sum-frequency generation process [15] and TPA of organic molecules [16]. The transition rate for classical light has a quadratic dependence on intensity, whereas that for entangled photons exhibits a linear dependence at low intensity, which is typically found in one-photon absorption. Thus, an entangled-photon pair acts as a single photon and realizes high TPA at low intensity.

In order to maximally enhance the two-photon transition rate by entangled photons, ultrashort-pulsed entangled photons, in other words, ultrabroadband frequency-entangled photons are desired. Fortunately, recent leading-edge experiments in the field of quantum optics enables the generation of such ultrabroadband frequency-entangled photons, and entangled photons with a frequency range of $\sim$ 160 THz [17] are experimentally obtained at present by using the chirped quasi-phase-matching technique [18]. However, at the same time, the wide bandwidth of entangled photons raises an emerging problem that the intermediate states, which are originally off resonant (virtual excitation), are really excited as a consequence of the broad frequency band. As a result, two-step excitation (TSE) via the real excitation of intermediate states dominates TPA. For application to molecular processes, this might be unfavorable because the chemical reaction depends on which vibronic states are excited. Therefore, the real excitation of intermediate states might decrease the quantum efficiency of a target molecular process induced in the excited state. Furthermore, the suppression of TSE can lead to application to virtual state spectroscopy [19].

In this paper, to avoid the real excitation of intermediate states, we introduce spectral holes for entangled photons and analyze in detail the two-photon process using spectrally shaped entangled photons. A spectral hole is introduced around the energy level of the intermediate state so that TSE via the real excitation of the intermediated state rarely occurs. Taking a cold Rb atom [20] as an example, we show that the spectral holes well suppress the real excitation of the intermediate state and recover the TPA via a virtual state. Furthermore, for a short pulse close to a monocycle, we show that, though spectral shaping slightly reduces the enhancement rate, the excitation efficiency can be enhanced a thousand times as large as that by uncorrelated photons.

The rest of this paper is organized as follows. In Sec. II, a theoretical model of a one-dimensional input-output system is introduced and the formulation of entangled-photon pairs with spectral holes is given. In Sec. III, we analyze in detail the quantum dynamics driven by spectrally shaped entangled-photon pairs and the dependence of TPA efficiency on pulse width. In Sec. IV, we summarize and discuss our results.

II. MODEL

A. One-dimensional atom model

As a theoretical model, we consider a one-dimensional photon field interacting with a three-level atom, as depicted in Fig. 1(a). An incident two-photon pulse propagates parallel to the r axis and interacts with the atom positioned at the origin. The details of the entangled photons and the atom are shown in Fig. 1(b). For entangled photons, a rectangular pulse

*h-oka@eng.niigata-u.ac.jp

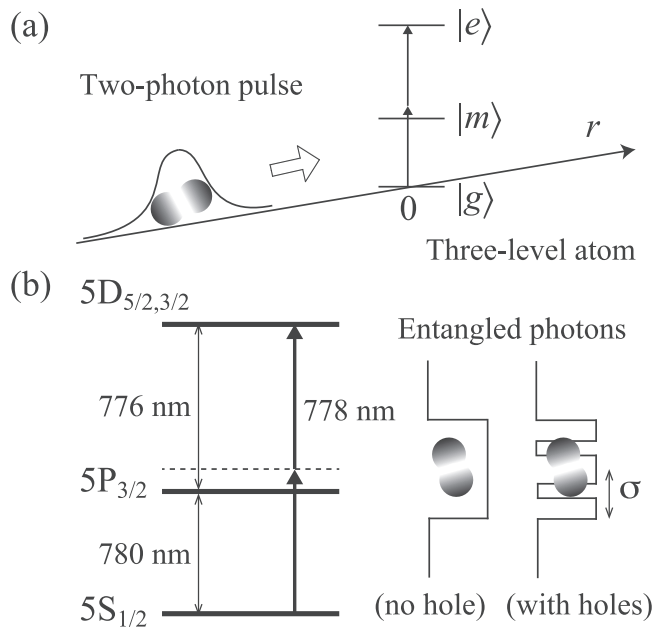

FIG. 1. (a) One-dimensional input-output model. (b) Schematic of TPA process in a Rb atom by entangled photons.

in the frequency domain is used by reference to Ref. [17]. For the atomic levels, we adopt the three levels of a Rb atom [20], namely, $5S^{1/2}$ for the ground state $|g\rangle$, $5P^{3/2}$ for the intermediate state $|m\rangle$, and $5D^{5/2,3/2}$ for the excited state $|e\rangle$. The transition wavelengths are 780 nm for $5S^{1/2} \rightarrow 5P^{3/2}$ ($|g\rangle \rightarrow |m\rangle$) and 776 nm for $5P^{3/2} \rightarrow 5D^{5/2,3/2}$ ($|m\rangle \rightarrow |e\rangle$). The central wavelength of incident photons is 778 nm so that two photons are resonant with the excited state $|e\rangle$. Spectral holes are introduced at wavelengths of 780 and 776 nm so that the spectral symmetry of the entangled photons is preserved.

B. Hamiltonian and quantum dynamics

Setting the natural units of $\hbar = c = 1$ and using the dispersion relation of $\omega = ck = k$, the Hamiltonian of the whole system is given by

$$\hat{H} = \int dk\, k\hat{a}^\dagger(k)\hat{a}(k) + \omega_e|e\rangle\langle e| + \omega_m|m\rangle\langle m| + \int dk(\gamma_m/\pi)^{1/2}[\hat{a}^\dagger(k)|g\rangle\langle m| + |m\rangle\langle g|\hat{a}(k)] + \int dk(\gamma_e/\pi)^{1/2}[\hat{a}^\dagger(k)|m\rangle\langle e| + |e\rangle\langle m|\hat{a}(k)], \quad (1)$$

where $\hat{a}(k)$ [$\hat{a}^\dagger(k)$] is the annihilation (creation) operator of a photon with energy k. γ_m and γ_e are the relaxation rates of $|m\rangle$ and $|e\rangle$, respectively. In this paper, we set $\gamma = \gamma_m = \gamma_e = 6$ MHz, for simplicity, and ignore the direct transition between $|g\rangle$ and $|e\rangle$ by one photon.

The dynamics of the whole system can be calculated from the Schrödinger equation,

$$\frac{d}{dt}|\Psi(t)\rangle = -i\hat{H}|\Psi(t)\rangle. \quad (2)$$

$|\Psi\rangle$ can be expressed as a superposition state, given by

$$|\Psi\rangle = 2^{-1/2}\int dk \int dk'\psi_{2p}(k,k')\hat{a}^\dagger(k)\hat{a}^\dagger(k')|0\rangle|g\rangle + \int dk\psi^m_{1p}(k)\hat{a}^\dagger(k)|0\rangle|m\rangle + \psi^e_0|0\rangle|e\rangle, \quad (3)$$

where $\psi_{2p}(k,k')$ is the two-photon joint amplitude of the incident pulse at $|g\rangle$, ψ^m_{1p} is the one-photon state at $|m\rangle$, and ψ^e_0 is the zero-photon state at $|e\rangle$. The argument t of ψ is omitted for simplicity. The initial state of the whole system $|\Psi(0)\rangle$ is given by the first term in Eq. (3), i.e., $\psi^m_{1p}(k) = \psi^e_0 = 0$, and the whole wave function is normalized to be $\langle\Psi|\Psi\rangle = 1$. From Eqs. (1)–(3), the Schrödinger equations for ψ can read

$$\frac{d}{dt}\psi_{2p}(k,k') = -i(k+k')\psi_{2p}(k,k') - i2^{-1/2}\Gamma_m\{\psi^m_{1p}(k) + \psi^m_{1p}(k')\}, \quad (4)$$

$$\frac{d}{dt}\psi^m_{1p}(k) = -i(k+\omega_m)\psi^m_{1p}(k) - i2^{1/2}\Gamma_m\int dk'\psi_{2p}(k,k') - i\Gamma_e\psi^e_0, \quad (5)$$

$$\frac{d}{dt}\psi^e_0 = -i\omega_e\psi^e_0 - i\Gamma_e\int dk\psi^m_{1p}(k), \quad (6)$$

where $\Gamma_m = (\gamma_m/\pi)^{1/2}$ and $\Gamma_e = (\gamma_e/\pi)^{1/2}$. Populations of atomic intermediate and excited states are calculated from $\langle e\rangle = |\langle e|\Psi(t)\rangle|^2$ and $\langle m\rangle = |\langle m|\Psi(t)\rangle|^2$, respectively.

C. Spectrally shaped entangled photons: Introduction of spectral holes

For comparison, we consider four photon pairs: an uncorrelated photon pair, an entangled photon pair with an energy anticorrelation, and the spectrally shaped photon pairs of uncorrelated and entangled photons. The uncorrelated photon pair, corresponding to classical light, is given by

$$\psi_{2p}(k,k') = \varphi(k)\varphi(k')e^{-ikr_0}e^{-ik'r_0}, \quad (7)$$

where $\varphi(k)$ is the one-photon wave packet in k representation and r_0 is the spatial center position of the wave packet at $t = 0$. In the uncorrelated photon pair, there is no correlation between the two photons and therefore the two-photon wave packet can be divided into the direct product of one-photon wave packets.

The entangled photon pair with an energy anticorrelation is given by

$$\psi_{2p}(k,k') = \varphi(k)\delta(k+k'-\omega_e)e^{-ikr_0}e^{-ik'r_0}. \quad (8)$$

This is referred to as the twin-beam state and can be obtained, e.g., from spontaneous parametric down-conversion. $\delta(k + k' - \omega_e)$ indicates the energy anticorrelation of two photons: One photon with energy $k = k_0 - \Delta$ is accompanied by the other photon with energy $k' = k_0 + \Delta$, conserving a total energy of $\omega_e = 2k_0$, where k_0 is the central energy of the photon pulse. By Fourier transforming to the time domain, this property implies that the photon pair inherently has a time coincidence.

The spectrally shaped photon pairs can be defined by imposing a limitation to $\varphi(k)$ and $\varphi(k')$ in Eqs. (7) and (8)

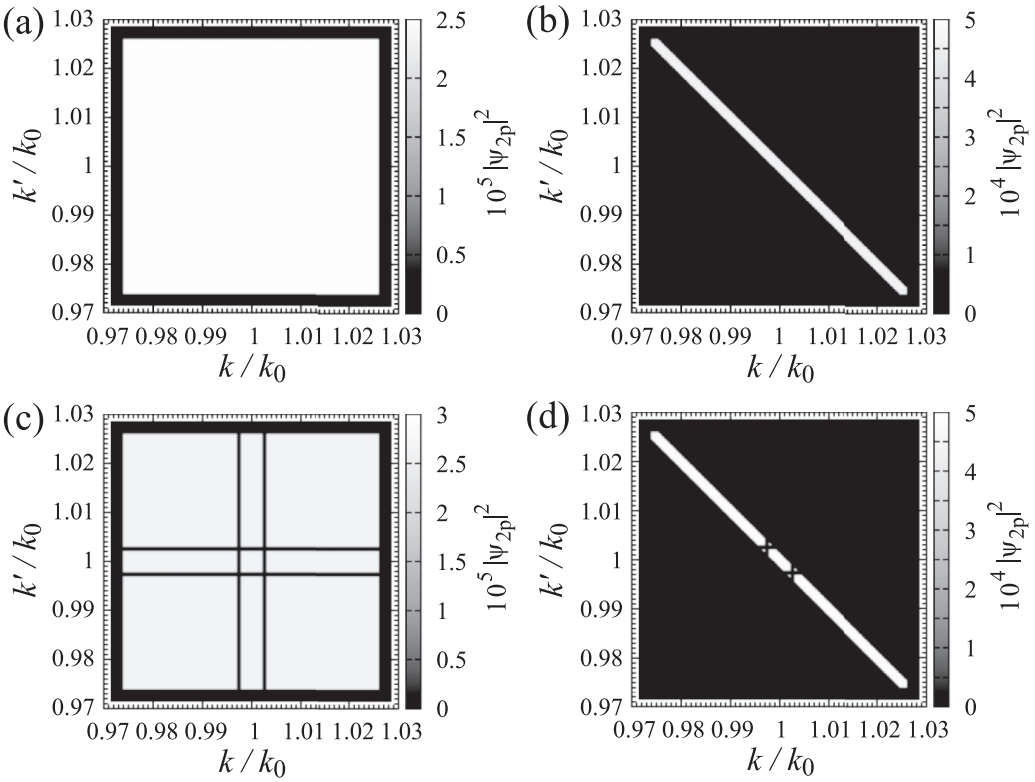

FIG. 2. Two-photon joint spectra $|\psi_{2p}|^2$: (a) Uncorrelated photons, (b) entangled photons, (c) uncorrelated photons with holes, and (d) entangled photons with holes. k and k' are normalized by the central energy of photons k_0.

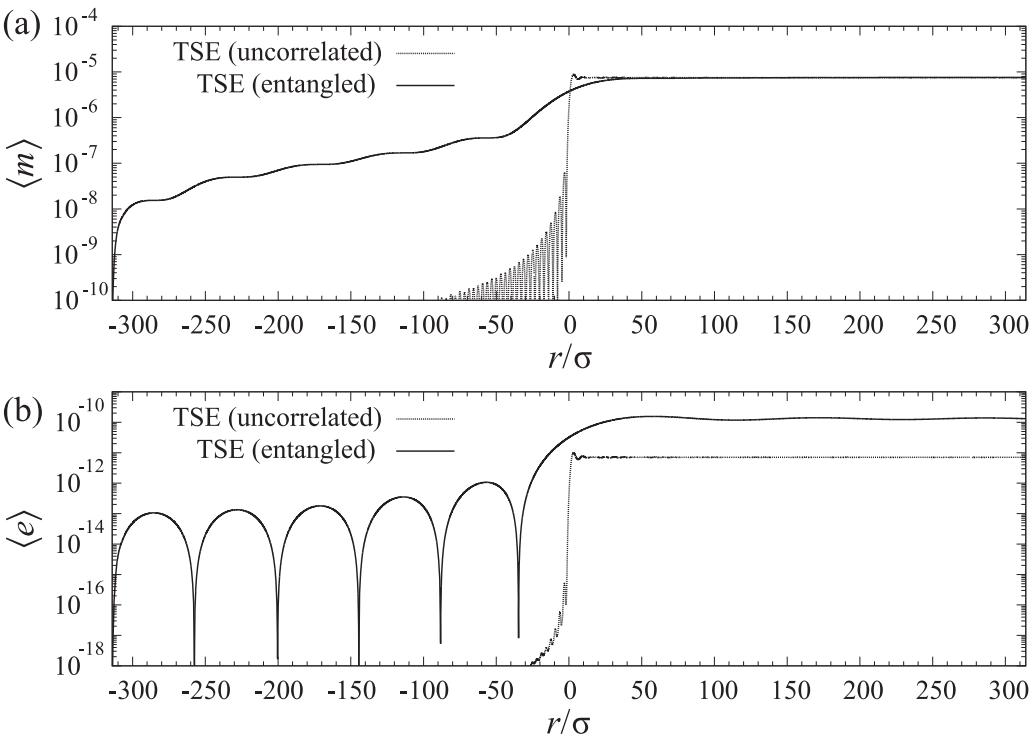

FIG. 3. TSE driven by uncorrelated and entangled photons with no holes as a function of r/σ: (a) $\langle m \rangle$ and (b) $\langle e \rangle$. The solid line is for entangled photons and the dotted line is for uncorrelated photons.

as

$$\varphi(k) = 0 \quad \text{for} \quad |k - \omega_m| \leqslant d \quad \text{and} \quad |k - \omega_e + \omega_m| \leqslant d, \quad (9)$$

where d is a width of the spectral hole. The second limitation of $|k - \omega_e + \omega_m| \leqslant d$ arises from the symmetric property of the two-photon wave function, $\psi_{2p}(k,k') = \psi_{2p}(k',k)$.

As mentioned in Sec. II A, we adopt a rectangular pulse in the frequency domain following Ref. [17]. The two-photon joint spectra $|\psi_{2p}(k,k')|^2$ for the four photon pairs are shown in Fig. 2, where $\sigma = 10$ THz and $d = 300$ GHz are used. The Dirac δ function in Eq. (8) is replaced by a rectangular function ϕ, defined as $\phi = 2\Delta k^{-1}$ for $|k + k' - \omega_e| \leqslant \Delta k$ and $\phi = 0$ for the other so that ϕ corresponds to the δ function in the limit of $\Delta k \to 0$. Intriguingly, the spectra of the entangled photon pairs are classically identical to those of the uncorrelated photon pair for $\Delta k \ll 1$. For the entangled-photon generation by parametric down-conversion, Δk is determined by the pulse width of the pump light. Therefore, if we use a cw narrow-spectrum laser, $\Delta k \approx 100$ kHz can be experimentally achieved. In Fig. 2, however, $\Delta k = 500$ GHz is used to reduce a computational task.

In the actual calculation of Eqs. (4)–(6), we omit the degrees of freedom of polarization by assuming linearly polarized light and solve the equations numerically by discretizing the photon fields. Concretely, continuous photon fields are discretized by converting from $(\delta k)^{-1} \int dk$ and $(\delta k)^{1/2}\hat{a}(k)$ to $\sum_k$ and $\hat{a}_k$, respectively, where $\delta k = 2\pi/L$ is the mode spacing and L is the length of calculation region. The two-photon joint spectrum is then transformed from $|\psi_{2p}(k,k')|^2 \delta k \delta k'$ to $|\psi_{k,k'}|^2$, where $\delta k \delta k'$ indicates the minimum unit of two-photon distribution. In this paper, $\delta k = 100$ GHz is used to reduce the computational task and the total number of photon modes is 4 844 401 (2201 modes per photon), which corresponds to 1.1 time of the full width of $\sigma = 100$ THz. The discretized Schrödinger equations can be solved, e.g., by using the Runge-Kutta method.

III. RESULTS

In this section, we analyze the two-photon excitation by spectrally shaped entangled photons, in terms of how the introduced spectral holes affect the two-photon excitation efficiency and how the excitation efficiency depends on the spectral width σ. The enhancement of excitation efficiency by entangled photons is evaluated by the population ratio ξ between the population $\langle e \rangle$ obtained from entangled photons and that obtained from uncorrelated photons.

We first calculate the quantum dynamics of two-photon excitation driven by spectrally shaped photon pairs. For comparison, the population dynamics for uncorrelated and entangled photons with no holes is shown in Fig. 3. The parameters are the same as those in Fig. 2 except for $d = 700$ GHz. The horizontal axis is the spatial center position r of the incident pulse, normalized by σ, and the vertical axis is the population of the atomic system, represented by the logarithmic scale. When an incident pulse reaches $r = 0$, the atomic system absorbs one photon and $|m\rangle$ is excited. Then, $|e\rangle$ is excited by absorbing the other photon, however, $\langle m \rangle$ remains constant and does not decrease for both uncorrelated and entangled photons. This is a well-known TSE process, where each photon is absorbed at $|m\rangle$ and $|e\rangle$ unlike in the case of TPA. Interestingly, $\langle e \rangle$ is enhanced approximately 30 times by entangled photons, whereas the population of $\langle m \rangle$ is the same for uncorrelated and entangled photons. This implies that the quantum entanglement between

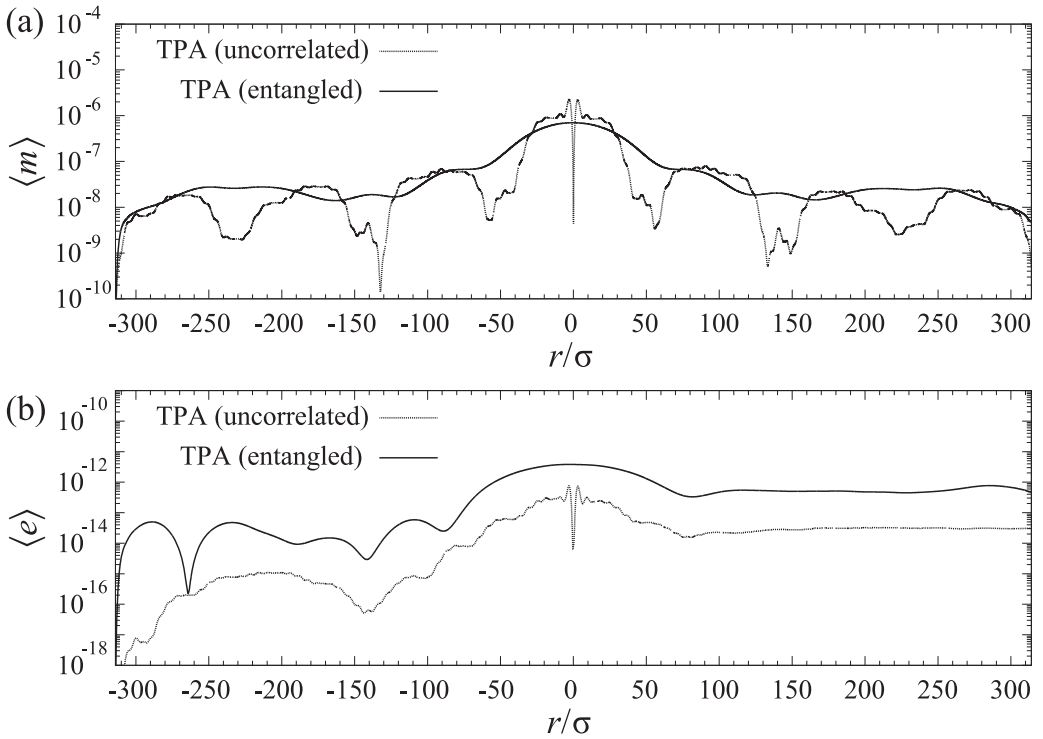

FIG. 4. TPA driven by uncorrelated and entangled photons with holes as a function of r/σ. The solid line is for entangled photons and the dotted line is for uncorrelated photons.

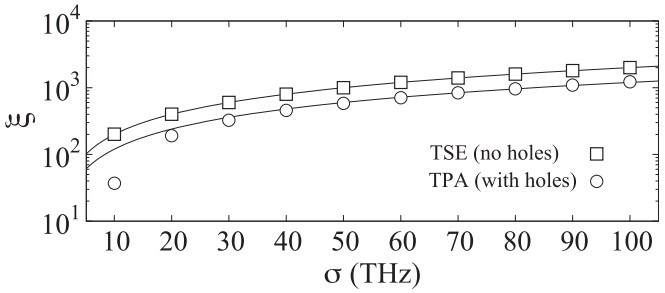

FIG. 5. ξ as a function of σ.

the two photons does not affect the one-photon absorption from $|g\rangle$ to $|m\rangle$.

Figure 4 shows the population dynamics for uncorrelated and entangled photons with holes. In the presence of holes, the population of $\langle m\rangle$ decreases drastically for both uncorrelated and entangled photons after the photon pulses pass by the atom. The sinc-function-like long-period oscillation found in $\langle m\rangle$ is due to rectangular holes in the k domain. Though the value of $\langle e\rangle$ is considerably smaller than that of TSE, $\langle e\rangle$ is enhanced approximately 17 times by entangled photons with holes. Thus, by introducing spectral holes into two-photon pulses, we can recover the TPA process by suppressing the real excitation of $\langle m\rangle$ and enhance the excitation efficiency of the TPA by using entangled photons.

According to previous studies [9,13], the enhancement ξ can be increased by both broadening the pulse width σ and strengthening the energy correlation between the two photons, corresponding to the narrowing of Δk ($\phi \to \delta$ function). Figure 5 shows the dependence of ξ on σ for the range from 10 to 100 THz. The parameters are the same as those in Figs. 3 and 4, except for σ and $\Delta k = 100$ GHz. In both TPA and TSE, ξ gradually increases as σ increases. For small $\sigma \leqslant 20$ THz, the enhancement ξ of TPA is considerably smaller than that of TSE: In the present parameters, $\xi = 37$ for TPA and $\xi = 200$ for TSE. However, for σ larger than 50 THz, the difference of ξ between TPA and TSE becomes small as σ increases, and ξ eventually becomes almost linear with respect to σ (the solid lines in Fig. 5). For example, at $2\sigma = 200$ THz, the ratio becomes ≈ 1.64 and there is no great distinction between TPA and TSE: $\xi \approx 1222$ for TPA and $\xi \approx 2000$ for TSE. Thus, the introduction of spectral holes into entangled photons has an insignificant effect on entanglement enhancement and proves useful, especially for large σ.

IV. SUMMARY AND DISCUSSION

In summary, we have analyzed the TPA using spectrally shaped entangled photons, where spectral holes are introduced into the entangled photons to avoid the real excitation of the intermediate state and to recover TPA from TSE. Taking the cold Rb atom as an example, we have shown that the TPA excitation efficiency can be enhanced a thousand times by short-pulsed entangled photons close to a monocycle pulse width of $2\sigma = 200$ THz. Thus, entangled photons with spectral holes are useful as a way to recover the TPA for atomic or molecular systems whose intermediate states exist near the central frequency of incident photons.

In this paper, we have focused on the two-photon excitations by exactly two photons in the limit of low intensity or low flux of incident light. Since the classical correlation dominates the quantum correlation between entangled photons at high intensity, we must enhance the efficiency of TPA at low intensity in order to maximally utilize the quantum nature of light. In addition, since the spectra of entangled photons, Eq. (8), are classically identical to those of the classical ones, Eq. (7), the only difference between Eqs. (7) and (8) is the quantum entanglement. Therefore, from the viewpoint of a theoretical analysis, the use of Eqs. (7) and (8) is quite reasonable. However, it might be difficult to experimentally compare the TPAs by these photon states, and hence the extension of theory to the number of detector counts might be useful for a comparison to experimental results. This will be our next step.

Throughout this paper, we have not mentioned the effects of relaxation rate γ on the TPA process. The excitation efficiency of TPA in low-intensity light, as considered in this paper, is primarily determined by γ of the target energy level, because the induced absorption of photons is negligibly small. Therefore, the population turns out to be low for atoms and molecules with small γ. Although we now utilize a high-intensity source of entangled photons, for a number of interesting molecular processes, highly intense light might lead to the deterioration and structural change of the molecules. Consequently, to achieve high excitation, we have to choose a specific material with γ. One possible way of avoiding this restriction is to utilize the nanoantenna effect as suggested in Ref. [14] and the cavity QED effects for molecules as in Ref. [21,22]. The former technique is summarized as the indirect enhancement of the absorption cross section of molecules using the antenna effect of nanoparticles and the latter is summarized as the direct enhancement of γ of molecules through cavity QED effects. With the use of a spectrally shaped entangled photon pair with large σ close to a monocycle, strong TPA enhancement in molecules could be expected. We hope that the results of this paper facilitate the applications of entangled photons to the chemical and biological fields, based on the TPA process.

ACKNOWLEDGMENTS

The author thanks Dr. M. Okano and Prof. Dr. S. Takeuchi for helpful advice. This work was supported by JSPS KAKENHI Grants No. JP15K04692 and No. JP17H05252 in Scientific Research on Innovative Areas "Photosynergetics," and CREST, JST.

[1] B. E. A. Saleh, B. M. Jost, H.-B. Fei, and M. C. Teich, Phys. Rev. Lett. **80**, 3483 (1998).

[2] O. Roslyak, C. A. Marx, and S. Mukamel, Phys. Rev. A **79**, 033832 (2009).

[3] M. G. Raymer, A. H. Marcus, J. R. Widom, and D. L. P. Vitullo, J. Phys. Chem. B **117**, 15559 (2013).
[4] F. Schlawin, K. E. Dorfman, and S. Mukamel, Phys. Rev. A **93**, 023807 (2016).
[5] K. E. Dorfman, F. Schlawin, and S. Makamel, Rev. Mod. Phys. **88**, 045008 (2016).
[6] F. Schlawin, J. Phys. B: At. Mol. Opt. Phys. **50**, 203001 (2017).
[7] M. B. Nasr, B. E. A. Saleh, A. V. Sergienko, and M. C. Teich, Phys. Rev. Lett. **91**, 083601 (2003).
[8] T. Ono, R. Okamoto, and S. Takeuchi, Nat. Commun. **4**, 2426 (2013).
[9] H. Oka, J. Chem. Phys. **134**, 124313 (2011).
[10] F. Schlawin and A. Buchleitner, New J. Phys. **19**, 013009 (2017).
[11] J. Gea-Banacloche, Phys. Rev. Lett. **62**, 1603 (1989).
[12] J. Javanainen and P. L. Gould, Phys. Rev. A **41**, 5088 (1990).
[13] H. Oka, Phys. Rev. A **81**, 053837 (2010).
[14] H. Oka, J. Phys. B: At. Mol. Opt. Phys. **48**, 115503 (2015).
[15] B. Dayan, A. Pe'er, A. A. Friesem, and Y. Silberberg, Phys. Rev. Lett. **94**, 043602 (2005).
[16] D.-I. Lee and T. Goodson III, J. Phys. Chem. B Lett. **110**, 25582 (2006).
[17] A. Tanaka, R. Okamoto, H.-H. Lim, S. Subashchandran, M. Okano, L. Zhang, L. Kang, J. Chen, P. Wu, T. Hirohata, S. Kurimura, and S. Takeuchi, Opt. Express **20**, 25228 (2012).
[18] S. E. Harris, Phys. Rev. Lett. **98**, 063602 (2007).
[19] R. de J. León-Montiel, J. Svozilík, L. J. Salazar-Serrano, and J. P. Torres, New J. Phys. **15**, 053023 (2013).
[20] S. M. Hendrickson, M. M. Lai, T. B. Pittman, and J. D. Franson, Phys. Rev. Lett. **105**, 173602 (2010).
[21] J. Flick, M. Ruggenthaler, H. Appel, and A. Rubio, Proc. Natl. Acad. Sci. USA **114**, 3026 (2017).
[22] M. Kowalewski and S. Mukamel, Proc. Natl. Acad. Sci. USA **114**, 3278 (2017).